JOC The Journal of Organic Chemistry

pubs.acs.org/joc Article

Computational Studies of Chiral Hydroxyl Carboxylic Acids: The Allylboration of Aldehydes

Elliot H. E. Farrar and Matthew N. Grayson*

Cite This: J. Org. Chem. 2020, 85, 15449−15456 Read Online

ACCESS | Metrics & More | Article Recommendations | Supporting Information

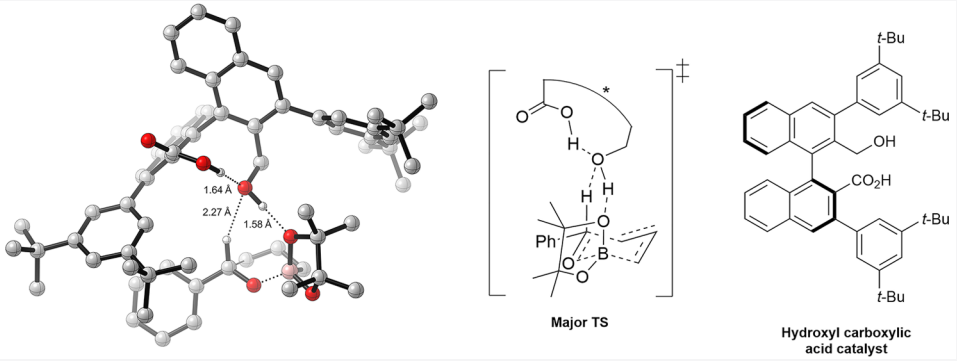

ABSTRACT: The mechanism of the asymmetric BINOL-derived hydroxyl carboxylic acid catalyzed allylboration of benzaldehyde was investigated using density functional theory calculations. A new reaction model is proposed, and the roles of the two Brønsted acidic sites of the catalyst elucidated. Catalyst distortion was found to be a key factor in determining stereoselectivity. The flexibility of the hydroxyl carboxylic acid catalyst leads to significant differences in the mechanism and origins of selectivity compared to the equivalent phosphoric acid catalyzed reaction.

INTRODUCTION

BINOL and its derivatives are one of the most popular groups of chiral catalysts in asymmetric organic synthesis.[1−3] Commonly used derivatives include phosphoric acids,[4,5] *N*-triflyl phosphoramides,[6] bis(sulfonyl)imides,[7,8] bis(sulfuryl)-imides,[9] and dicarboxylic acids.[10] BINOL-derived hydroxyl carboxylic acids (BHCAs) have seen increasing use in a variety of important asymmetric synthetic processes since 2015, including the fluorolactonization of vinylbenzoic acids[11] and C−C bond-forming reactions such as aldehyde allylboration and propargylation,[12] which are important methods in natural product syntheses.[13,14]

Although BHCAs are a relatively new and promising Brønsted acid catalyst, no detailed computational studies have been performed for any BHCA-catalyzed reaction. Such analyses could allow the optimization and development of new methodology for the broader use of BHCAs as catalysts in asymmetric synthesis. As a well-explored reaction type, allylboration marks an ideal case for investigations into the general workings of BHCAs as catalysts and allows comparisons to be made with the analogous BINOL-derived phosphoric acid (BPA)-catalyzed allylboration,[15] whose mechanism has seen extensive computational study.[16−19]

Asymmetric aldehyde allylboration is known to proceed via a cyclic, six-membered chairlike transition state structure (TS), where the boronate acts as a Lewis acid and activates the electrophile by its electron-deficient boron atom.[20,21] Quasi-classical direct molecular dynamics simulations have suggested that the boronate ester oxygen becomes partially negatively charged in the transition state as the boronate bonds to the aldehyde oxygen, enhancing the hydrogen bond accepting ability of the boronate oxygen and the hydrogen bond donating ability of the formyl hydrogen.[22] This leads to a stabilizing interaction between a Brønsted acidic site of the catalyst and boronate oxygen, as well as a stabilizing nonclassical (C−H···O) hydrogen bonding interaction between a Lewis basic site of the catalyst and the formyl hydrogen (Figure 1). The strength of this type of interaction was previously calculated using QM methods to be approximately 4.6 kcal·mol^{-1} with phosphoric acids.[22] Non-classical hydrogen bonding of this nature is a common phenomenon in asymmetric catalysis,[23] and a variety of organic transformations have had their selectivity rationalized on the basis of such interactions.[17,24,25] Our previous QM/MM

Received: September 15, 2020
Published: November 23, 2020

https://dx.doi.org/10.1021/acs.joc.0c02226
J. Org. Chem. 2020, 85, 15449−15456

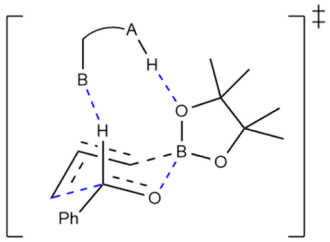

Figure 1. Key interactions in the acid catalyzed allylboration transition state structure.

studies on BPA-catalyzed allylboration support such a reaction model, with the BPA catalyst's hydroxyl group shown to interact with the pseudoaxial oxygen of the boronate (Figure 2, mode A).[17] An alternative mode, involving pseudoequatorial boronate protonation and no formyl interaction (Figure 2, mode B), has previously been suggested,[15,19,26] but was found to be disfavored in comparison to mode A.[17]

In accordance with the previous literature, Ota et al., in the original experimental report of BHCA-catalyzed allylboration, proposed that promotion of the reaction most likely occurs through enhancement of the Lewis acidity of the boronate via protonation of one of its oxygen atoms by one of the catalyst Brønsted acidic sites.[12] Additionally, Ota et al. found that the presence of both the carboxyl and alcohol functionalities at their respective positions of the BHCA catalyst were essential to the enantioselectivity of the reaction. However, although Ota et al. identified that hydrogen bonding between these two groups was likely to be important in the TS, the exact role of the alcohol group was not elucidated. Herein, we report density functional theory (DFT) calculations[27−30] (full details in Supporting Information (SI), Section 1) that have allowed us to analyze the propositions made by Ota et al. and determine the mechanism of the BHCA-catalyzed allylboration of aldehydes. The experimental conditions chosen for computational analysis are summarized in Figure 3.[12]

RESULTS AND DISCUSSION

In total, 145 unique TSs were obtained for the catalyzed reaction (full details in SI, Section 5), of which the lowest in energy, **TS-2.1**, yields a $\Delta G^{\ddagger}$ value of 4.1 kcal·mol^{-1} (Figure 4), 13.1 kcal·mol^{-1} lower than the respective value calculated for the uncatalyzed pathway via **TS-1**$_{\text{chair-eq}}$ (see SI, Section 4). The lowest-energy TS leading to the minor product, **TS-2.2**, is

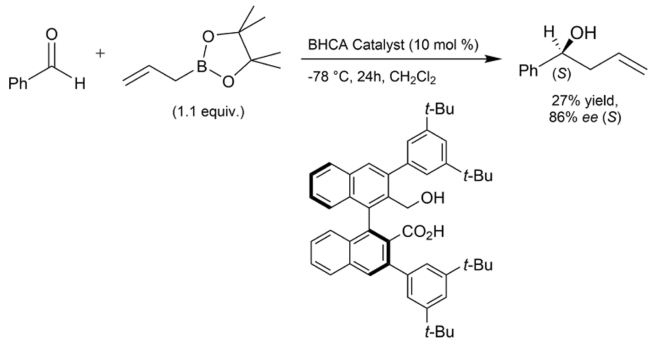

Figure 3. BHCA-catalyzed allylboration.

0.7 kcal·mol^{-1} higher in energy than **TS-2.1** (Figure 4). Based on a Boltzmann weighting at 195.15 K over all conformers within 3.0 kcal·mol^{-1} of **TS-2.1**, a computed *ee* of 79% was predicted, in excellent agreement with the experimental *ee* of 86%.

Intramolecular hydrogen bonding was observed between the carboxyl and alcohol groups of the catalyst for all TSs within 7.3 kcal·mol^{-1} of **TS-2.1**. In the absence of such hydrogen bonding, a 0.5 kcal·mol^{-1} difference in energy was found between the lowest major and minor TSs, corresponding to a computed *ee* of 57%. Thus, by reducing the degree of rotational freedom about the bond connecting the catalyst acid moiety to the chiral scaffold, this intramolecular hydrogen bonding allows for a better transfer of chiral information and hence higher asymmetric induction by the catalyst. The carboxyl group was found to be the preferred hydrogen bond donor in favor of the alcohol group; **TS-2.4**, the lowest-energy TS, where the alcohol group acts as the hydrogen bond donor, is 4.1 kcal·mol^{-1} higher in energy than **TS-2.1** (Figure 5). The same trend was observed in the lowest-energy structure of the isolated catalyst, where the carboxyl group also acts as the hydrogen bond donor. The lowest-energy catalyst structure where the alcohol group acts as the hydrogen bond donor is 1.3 kcal·mol^{-1} higher in energy (Figure S1). This trend may be rationalized by the relative acidities of the two groups, with the carboxyl group being more acidic and hence a better hydrogen bond donor.

A mix of pseudoaxial and pseudoequatorial boronate oxygen protonation by the catalyst was observed, with the protonating group determined by the type of intramolecular bonding in the

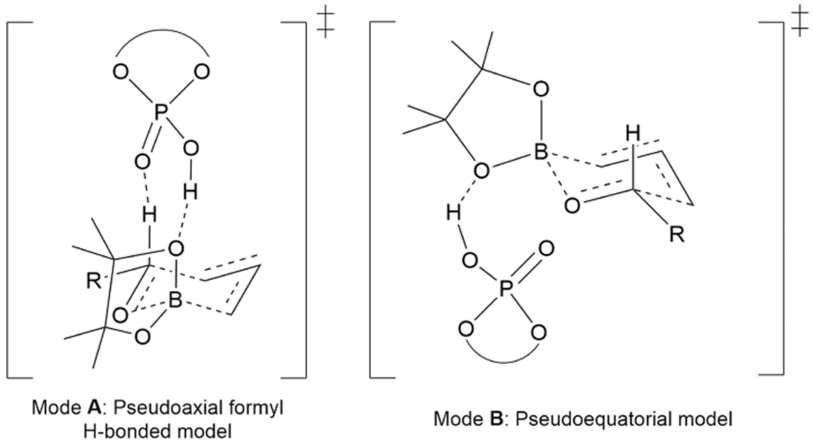

Figure 2. Reactions models for BPA-catalyzed allylboration.

https://dx.doi.org/10.1021/acs.joc.0c02226
J. Org. Chem. 2020, 85, 15449−15456

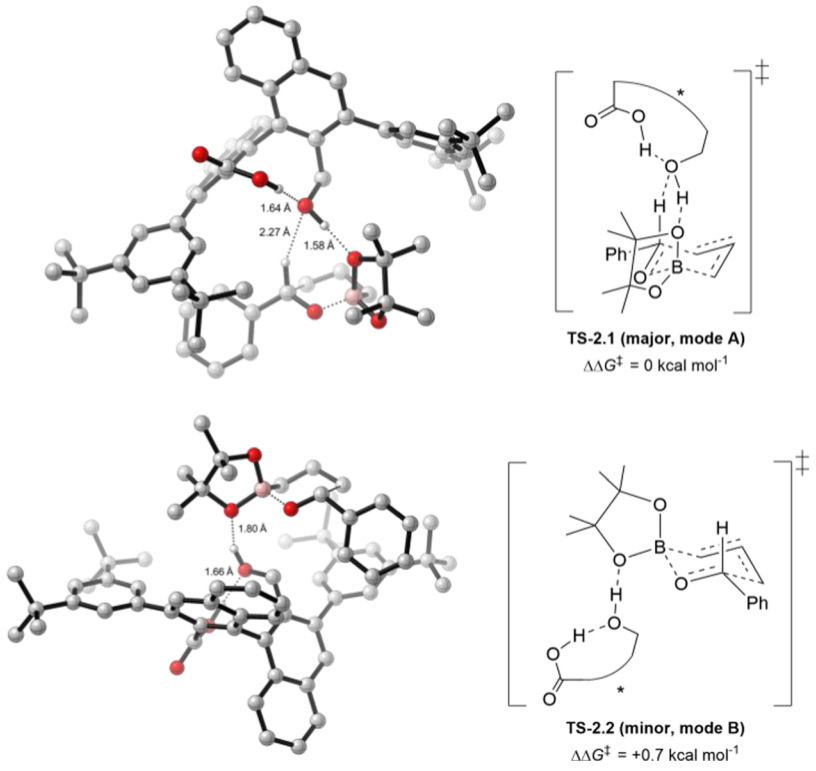

Figure 4. Lowest-energy major (**TS-2.1**) and minor (**TS-2.2**) TSs for BHCA-catalyzed allylboration. Energies relative to **TS-2.1** (B3LYP-D3(BJ)/def2-TZVPP/IEF-PCM(dichloromethane)//B3LYP-D3(BJ)/6-31G(d,p)).

catalyst; when the carboxyl group acts as the hydrogen bond donor, the alcohol group is left free to protonate the boronate oxygen and vice versa. Hence, protonation of the boronate oxygen occurs via the alcohol group in all TSs within 4.1 kcal·mol^{-1} of **TS-2.1**, and all catalysts within 1.3 kcal·mol^{-1} of the lowest-energy catalyst structure. It may be expected that protonation of the boronate oxygen by the more acidic carboxyl group, with the alcohol group acting as the intramolecular hydrogen bond donor, as in **TS-2.4** or **TS-2.5** (Figure 5), the lowest-energy mode B and mode A structures of this type, respectively, should be preferred, as they would activate the boronate more strongly and thus catalyze the reaction more effectively. However, TSs of this nature were found to result in a significantly greater distortion of the catalyst away from its optimum geometry, resulting in their higher energy. The origins and effects of this catalyst distortion are discussed below. The magnitude of this distortion is larger in the transition state than in the isolated catalyst due to additional distortion of the catalyst aryl groups to avoid steric clashing with the substrate. This explains why there is a greater preference for the carboxyl group to act as the intramolecular hydrogen bond donor in the transition state (4.1 and 6.6 kcal·mol^{-1}) than in the catalyst (1.3 kcal·mol^{-1}).

In contrast to our previous work on BPA-catalyzed allylboration,[17] where both the lowest-energy major and minor TSs were found to proceed via the same pseudoaxial formyl H-bonded TS model (Figure 2, mode A), **TS-2.1** and **TS-2.2** are distinctly different in their activation modes. Whereas **TS-2.1** corresponds to this formyl H-bonded model, possessing both a nonclassical hydrogen bonding interaction between the Lewis basic alcohol oxygen and the acidic formyl proton, and pseudoaxial boronate oxygen protonation by the acidic alcohol group, **TS-2.2** corresponds to the pseudoequatorial TS model (Figure 2, mode B). This involves a six-membered chairlike TS with the activation of the pseudoequatorial boronate oxygen via protonation by the catalyst alcohol group and no formyl interaction. The lowest-energy mode A TS corresponding to the formation of the minor enantiomer of the product, **TS-2.3**, is 1.9 kcal·mol^{-1} higher in energy than **TS-2.1** (Figure 6).

Under mode A, enantioselectivity in the BPA-catalyzed allylboration was rationalized based on steric factors related to the boronate pinacol ester methyl groups and the aldehyde substituent, with the steric demand of the former found to outweigh that of the latter.[17] Hence, the major enantiomer of the product results from whichever TS is able to place the pinacol ester methyl groups in the sterically less demanding pocket of the catalyst at the expense of the aldehyde substituent. No H−H contacts between the substrate and catalyst within 90% of the van der Waals radii were found in **TS-2.1**, **TS-2.2**, or **TS-2.3**, suggesting that there is no significant steric clash between the substrate and catalyst in any case. As a result, it is not possible to rationalize the enantioselectivity for the BHCA-catalyzed allylboration based on steric factors.

A detailed conformational analysis of the two catalytic species found BHCAs to be significantly more flexible than their phosphoric acid counterparts, with 31 conformations generated following DFT optimization of a simple BHCA species, compared to only two for the corresponding BPA (Figure 7). Although both species possess a central atom (C and P, respectively) with a Brønsted acidic site (carboxylic or phosphoric hydroxyl group, respectively) and a Lewis basic site (double bond to oxygen), BHCAs also possess an alternative Brønsted acidic site in the alcohol group, which is not tethered to the same atom as the Lewis basic carbonyl oxygen, as in

https://dx.doi.org/10.1021/acs.joc.0c02226
J. Org. Chem. 2020, 85, 15449−15456

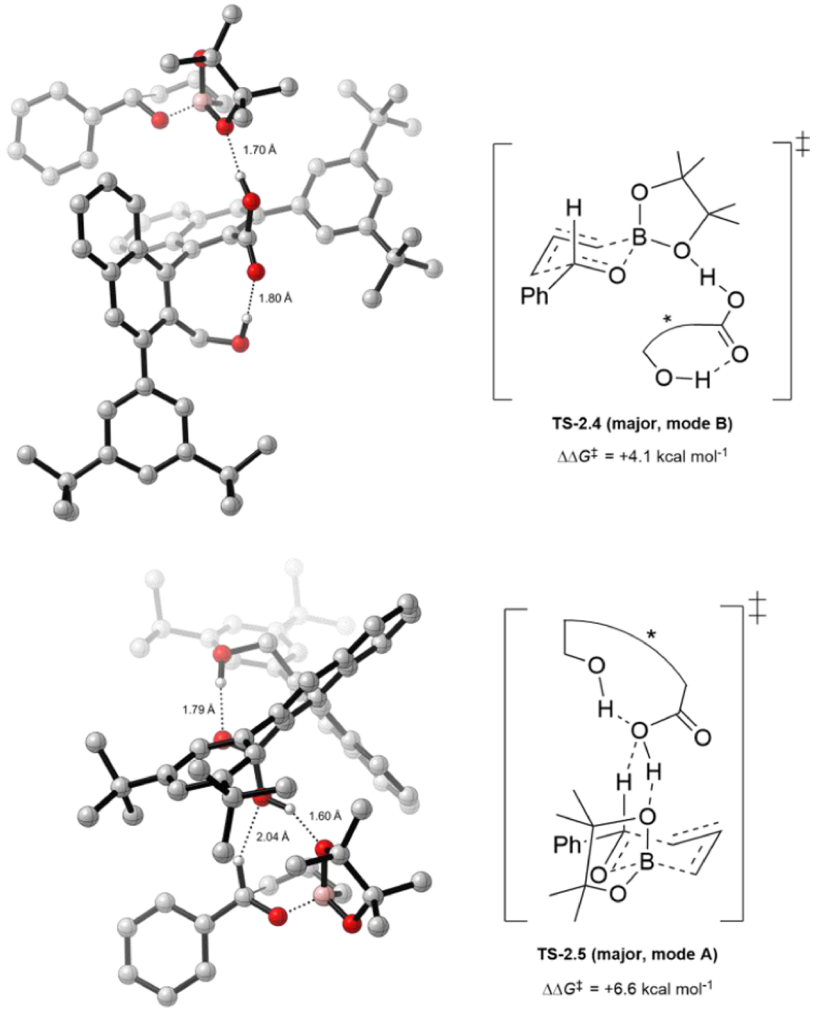

Figure 5. Lowest-energy mode B (**TS-2.4**) and mode A (**TS-2.5**) TSs for BHCA-catalyzed allylboration where the alcohol and carboxyl groups act as the hydrogen bond donor and acceptor, respectively. Energies relative to **TS-2.1** (B3LYP-D3(BJ)/def2-TZVPP/IEF-PCM(dichloromethane)//B3LYP-D3(BJ)/6-31G(d,p)).

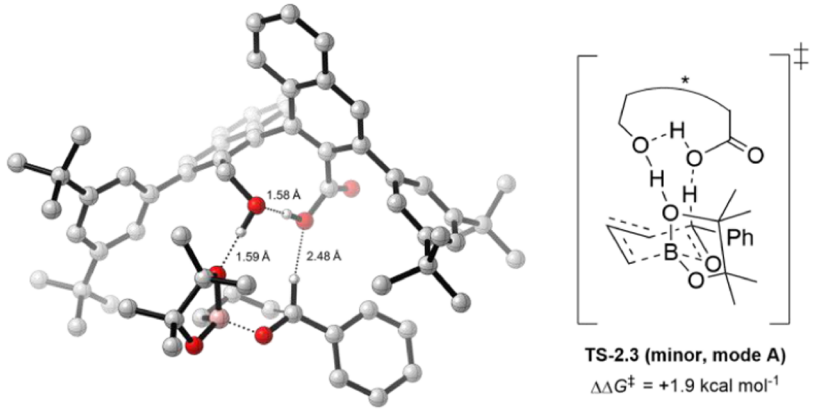

Figure 6. Lowest-energy mode A minor TS for BHCA-catalyzed allylboration. Energy relative to **TS-2.1** (B3LYP-D3(BJ)/def2-TZVPP/IEF-PCM(dichloromethane)//B3LYP-D3(BJ)/6-31G(d,p)).

BPAs, and is hence more conformationally flexible. As a result, the functional groups of the BHCA can exhibit a larger range of positions, resulting in many unique conformations. Conversely, the two BPA conformations result from the rotation of the phenyl groups, with no flexibility associated with the acid functionality. Additionally, BHCAs possess a flexible hydrogen-bonded structure,[31] in contrast to the cyclic O−P−O covalent bonding that rigidly links the phosphoric acid to the chiral scaffold in BPAs. This allows for a much larger range of dihedral angles about the BINOL C−C single bond than in BPAs.

https://dx.doi.org/10.1021/acs.joc.0c02226
J. Org. Chem. 2020, 85, 15449−15456

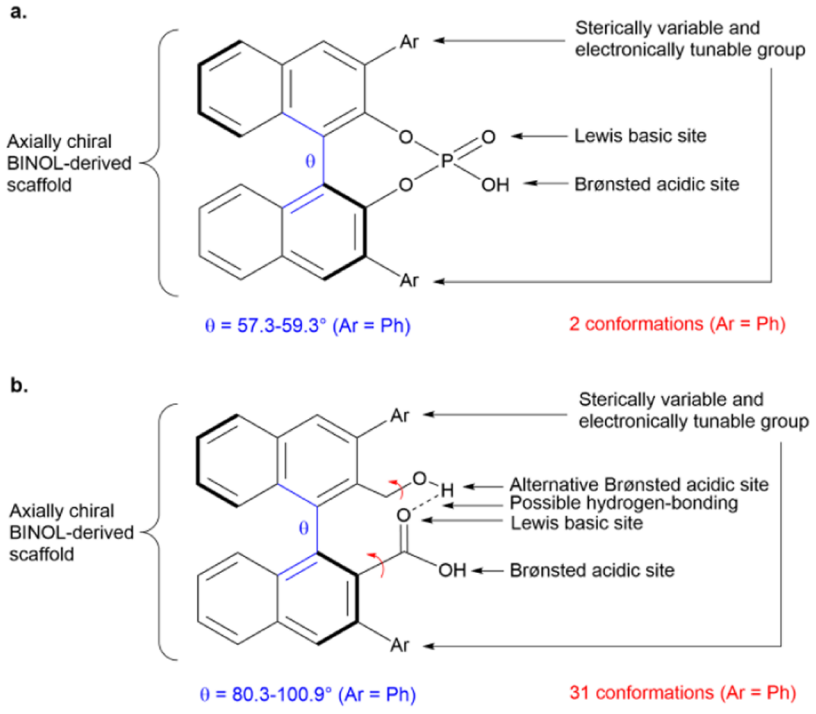

Figure 7. Major structural features and conformational analysis results of (a) BPAs and (b) BHCAs (B3LYP-D3(BJ)/def2-TZVPP/IEF-PCM(dichloromethane)//B3LYP-D3(BJ)/6-31G(d,p)).

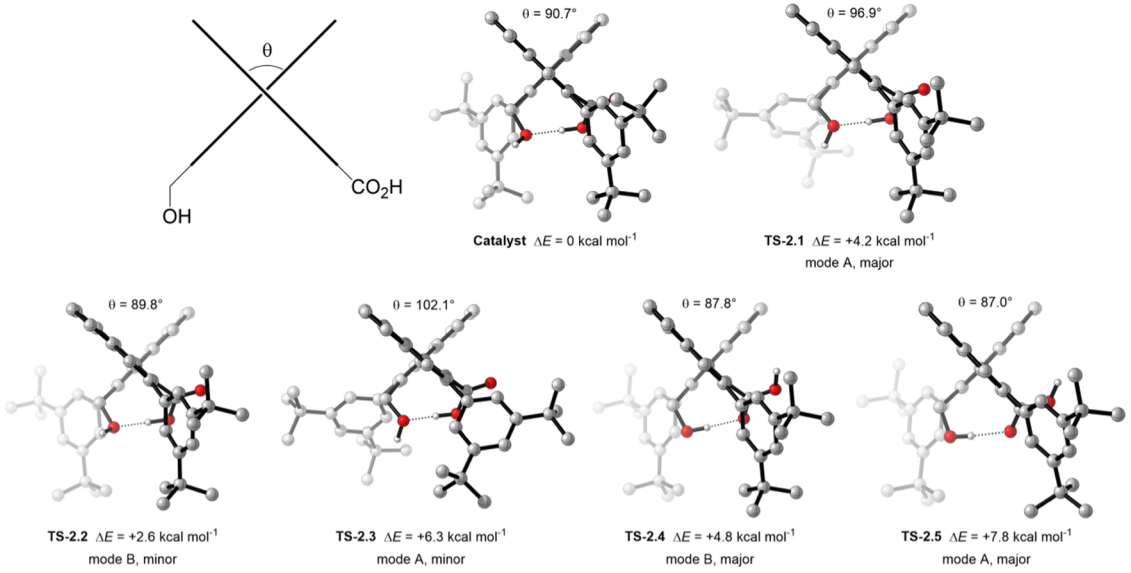

Figure 8. Dihedral angle and degree of distortion for each of the catalyst structures within **TS-2.1**, **TS-2.2**, **TS-2.3**, **TS-2.4**, and **TS-2.5**, compared to the optimum isolated catalyst geometry (B3LYP-D3(BJ)/def2-TZVPP/IEF-PCM(dichloromethane)).

This additional flexibility is key to determining the mechanistic differences between the two acid catalyzed allylboration reactions. As a result of this flexibility, the BHCA catalyst is able to adjust its structure and bind the substrate in such a way that allows both the pinacol ester methyl groups and aldehyde substituent to avoid steric interactions with the catalyst, whilst still forming tight interactions with the boronate oxygen and formyl proton. Such an adaptation is not possible for the more rigid BPA catalyst, where the Brønsted acidic and the Lewis basic sites are covalently bound to one another. However, by adjusting its structure like this, the BHCA catalyst is distorted and destabilized relative to its optimum geometry. Close inspection of **TS-2.1**, **TS-2.2**, **TS-2.3**, **TS-2.4**, and **TS-2.5** revealed that changes in the BINOL C−C dihedral angle of the catalyst structures are a major source of this distortion, whilst SPE calculations of the isolated catalyst structures from these TSs helped to quantify the relative extents of distortion (Figure 8). Interaction lengths, given in brackets where appropriate, provide further insight into the energetic trends of the five TSs.

TS-2.2 was found to possess the least destabilized catalyst structure relative to the optimum catalyst structure, likely due to the single-point substrate−catalyst binding in mode B, minimizing the potential for steric clashing and hence the

https://dx.doi.org/10.1021/acs.joc.0c02226
J. Org. Chem. 2020, 85, 15449−15456

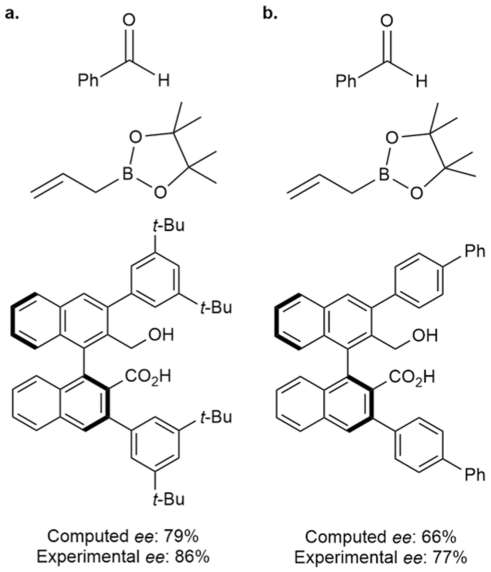

Figure 9. (a) Original conditions and (b) alternative catalyst. Both with 10% mol catalyst, −78 °C, 24 h, CH_2Cl_2.

extent of distortion. For the mode A TSs, **TS-2.5** possesses the most destabilized catalyst structure, followed by **TS-2.3** and then **TS-2.1**. However, **TS-2.1**, despite possessing a more destabilized catalyst structure than **TS-2.2**, is an overall lower-energy TS. This may be rationalized by the presence of the electronically stabilizing formyl C−H···O interaction (2.27 Å) and the tighter binding of the boronate oxygen (1.58 Å vs 1.80 Å) in **TS-2.1**, which compensates for the greater distortion relative to **TS-2.2** ($\Delta\Delta E$ = +1.6 kcal·mol^{-1}). Like **TS-2.1**, **TS-2.3** also exhibits an electronically stabilizing formyl interaction (2.48 Å) and a tighter binding of the boronate oxygen compared to **TS-2.2** (1.59 Å vs 1.80 Å) but is a higher-energy TS than **TS-2.2** for the formation of the minor enantiomer. This is partially rationalized by the catalyst structure in **TS-2.3** being significantly more distorted than that in **TS-2.2** ($\Delta\Delta E$ = +3.7 kcal·mol^{-1}). Furthermore, as a result of this additional distortion, the Brønsted acidic sites of the catalyst in **TS-2.3** are positioned less optimally than those in **TS-2.1**. Thus, it is not possible for the alcohol group of the catalyst to both protonate the boronate oxygen and interact with the formyl proton, as in **TS-2.1**, and so interaction with the formyl proton instead occurs via the carboxyl group, while the alcohol group protonates the boronate. As a result, the electronically stabilizing formyl interaction in **TS-2.3** (2.48 Å, calculated at 0.7 kcal·mol^{-1} by NBO analysis) is longer, and thus less electronically stabilizing, than the corresponding interaction in **TS-2.1** (2.27 Å, calculated at 2.5 kcal·mol^{-1} by NBO analysis). This further explains why **TS-2.3** cannot compensate for the greater catalyst distortion relative to **TS-2.2**. The significant catalyst distortion in **TS-2.4** and **TS-2.5**, where the carboxyl group protonates the boronate oxygen and the alcohol group acts as the intramolecular hydrogen bond donor, results in the significantly higher energy of TSs of this nature.

To explore the generality of our reaction model, all computed TSs within 3.0 kcal·mol^{-1} of **TS-2.1** were reoptimized using an alternative catalyst from the original experimental paper (Figure 9).[12] The computed structures for this new system were Boltzmann weighted at 195.15 K over all conformers, resulting in a predicted *ee* of 66%, in strong agreement with the experimental *ee* of 77%. Low-energy TSs analogous to **TS-2.1**, **TS-2.2**, and **TS-2.3**, denoted by a prime, were all identified (Figure S8); however, while **TS-2.1′** remains the major TS, **TS-2.3′** is found to be the lowest-energy minor TS. An investigation into the extent of catalyst distortion of each of these key TSs revealed that the new catalyst is less distorted in mode A TSs, compared to the original catalyst, but more distorted in mode B TSs (Table 1). Accordingly, the dihedral angle about the BINOL C−C single bond is closer to its optimum for the new catalyst in mode A TSs, compared to the original catalyst, but further away in mode B TSs. This is because the *para*-phenyl group of the new catalyst is less sterically demanding than the bulky meta-*t*Bu substituents of the original catalyst. In mode A TSs, this *para*-phenyl group lies away from the substrate and hence reduces the potential for substrate−catalyst steric clashing and allows the catalyst to relax closer to its optimum geometry. In accordance with these trends in catalyst distortion, **TS-2.3′** decreases by 1.1 kcal·mol^{-1} in free energy for the new catalyst relative to **TS-2.1′** and becomes the dominant pathway for the formation of the minor enantiomer of the product. In contrast, **TS-2.2′** increases by 0.2 kcal·mol^{-1} in free energy, compared to **TS-2.1′**. These changes correspond to the overall decrease in enantioselectivity observed experimentally.

CONCLUSIONS

The experimental results reported by Ota et al.[12] have been reproduced computationally, and insights into the BHCA-catalyzed allylboration mechanism and the general workings of BHCAs as catalysts obtained. The occurrence of intramolecular hydrogen bonding between the catalyst groups has been confirmed, with the more acidic carboxyl group found to be the favored hydrogen bond donor in preference to the alcohol group, which was instead found to protonate a boronate oxygen. These observations were rationalized in terms of the relative acidities of the Brønsted acidic groups. A formyl interaction between the Brønsted acidic sites of the catalyst and the formyl proton of the aldehyde was observed in some of the catalyzed reaction TSs, including the lowest-energy TS. Thus, the importance and individual roles of the

Table 1. Summary of Dihedral Angle and Degree of Catalyst Distortion, Relative to the Isolated Catalyst, in TS-2.1, TS-2.2, and TS-2.3 for the Original and Alternative Conditions (B3LYP-D3(BJ)/def2-TZVPP/IEF-PCM(dichloromethane))[a]

			original catalyst (Ar = 3,5-*t*Bu)			alternative catalyst (Ar = 4-Ph)		
structure	product	mode	catalyst distortion (ΔE)	C−C BINOL dihedral angle	relative free energy ($\Delta\Delta G^{\ddagger}$)	catalyst distortion (ΔE)	C−C BINOL dihedral angle	relative free energy ($\Delta\Delta G^{\ddagger}$)
TS-2.1	major	A	4.2	96.9	0.0	2.9	92.8	0.0
TS-2.2	minor	B	2.6	89.8	0.7	3.7	95.3	0.9
TS-2.3	minor	A	6.3	102.1	1.9	4.9	99.6	0.8

[a]All energies in kcal·mol^{-1}.

https://dx.doi.org/10.1021/acs.joc.0c02226
J. Org. Chem. 2020, 85, 15449−15456

alcohol and carboxyl groups of the catalyst were elucidated. The lowest-energy major TS resembled the pseudoaxial formyl H-bonded model (mode A), while the lowest-energy minor TS resembled a pseudoequatorial TS model (mode B). However, while the substrate−catalyst steric clashes dictated the selectivity of the BPA-catalyzed allylboration, any such steric clashes were avoided in the BHCA-catalyzed reaction as a result of the more flexible catalyst. Instead, the difference in energy between the TSs was the result of weaker substrate−catalyst interactions and catalyst distortion. An exploration of this TS system with an alternative catalyst helped to validate the results of the original calculations, with the relative extent of catalyst distortion remaining an important factor in selectivity.

■ ASSOCIATED CONTENT

Supporting Information

The Supporting Information is available free of charge at https://pubs.acs.org/doi/10.1021/acs.joc.0c02226.

Computational methods; complete list of authors for Gaussian09 and Gaussian16; ground-state structure; uncatalyzed reaction; and catalyzed reaction investigations; complete list of all energies; frequencies and molecular geometries (Cartesian coordinates) for all computed structures; and all Cartesian coordinates generated by the EsiGen software[32] (PDF)

■ AUTHOR INFORMATION

Corresponding Author

Matthew N. Grayson − *Department of Chemistry, University of Bath, Bath BA2 7AY, U.K.;* orcid.org/0000-0003-2116-7929; Email: M.N.Grayson@bath.ac.uk

Author

Elliot H. E. Farrar − *Department of Chemistry, University of Bath, Bath BA2 7AY, U.K.;* orcid.org/0000-0003-3350-2907

Complete contact information is available at: https://pubs.acs.org/10.1021/acs.joc.0c02226

Author Contributions

The manuscript was written through contributions of all authors. All authors have given approval to the final version of the manuscript.

Notes

The authors declare no competing financial interest.

■ ACKNOWLEDGMENTS

This research made use of the Balena High Performance Computing (HPC) Service at the University of Bath. Part of this work was performed using the resources provided by the Cambridge Service for Data Driven Discovery (CSD3) operated by the University of Cambridge Research Computing Service (http://www.csd3.cam.ac.uk/), provided by Dell EMC and Intel using Tier-2 funding from the Engineering and Physical Sciences Research Council (capital grant EP/P020259/1), and DiRAC funding from the Science and Technology Facilities Council (www.dirac.ac.uk). Prof. Jonathan Goodman is thanked for his support and helpful discussions regarding this work. The authors thank the EPSRC (studentship to E.H.E.F.) and the University of Bath for funding.

■ REFERENCES

(1) Pu, L. 1,1′-Binaphthyl Dimers, Oligomers, and Polymers: Molecular Recognition, Asymmetric Catalysis, and New Materials. *Chem. Rev.* **1998**, *98*, 2405−2494.

(2) Brunel, J. M. BINOL: A Versatile Chiral Reagent. *Chem. Rev.* **2005**, *105*, 857−898.

(3) Sedgwick, D. M.; Grayson, M. N.; Fustero, S.; Barrio, P. Recent Developments and Applications of the Chiral Brønsted Acid Catalyzed Allylboration of Carbonyl Compounds. *Synthesis* **2018**, *50*, 1935−1957.

(4) Uraguchi, D.; Terada, M. Chiral Brønsted Acid-Catalyzed Direct Mannich Reactions via Electrophilic Activation. *J. Am. Chem. Soc.* **2004**, *126*, 5356−5357.

(5) Yamanaka, M.; Itoh, J.; Fuchibe, K.; Akiyama, T. Chiral Brønsted Acid Catalyzed Enantioselective Mannich-Type Reaction. *J. Am. Chem. Soc.* **2007**, *129*, 6756−6764.

(6) Nakashima, D.; Yamamoto, H. Design of Chiral N-Triflyl Phosphoramide as a Strong Chiral Brønsted Acid and Its Application to Asymmetric Diels−Alder Reaction. *J. Am. Chem. Soc.* **2006**, *128*, 9626−9627.

(7) García-García, P.; Lay, F.; García-García, P.; Rabalakos, C.; List, B. A Powerful Chiral Counteranion Motif for Asymmetric Catalysis. *Angew. Chem., Int. Ed.* **2009**, *48*, 4363−4366.

(8) Treskow, M.; Neudörfl, J.; Giernoth, R. BINBAM - A New Motif for Strong and Chiral Brønsted Acids. *Eur. J. Org. Chem.* **2009**, *2009*, 3693−3697.

(9) Berkessel, A.; Christ, P.; Leconte, N.; Neudörfl, J.-M.; Schäfer, M. Synthesis and Structural Characterization of a New Class of Strong Chiral Brønsted Acids: 1,1′-Binaphthyl-2,2′-Bis(Sulfuryl)Imides (JINGLEs). *Eur. J. Org. Chem.* **2010**, *2010*, 5165−5170.

(10) Hashimoto, T.; Maruoka, K. Design of Axially Chiral Dicarboxylic Acid for Asymmetric Mannich Reaction of Arylaldehyde N-Boc Imines and Diazo Compounds. *J. Am. Chem. Soc.* **2007**, *129*, 10054−10055.

(11) Egami, H.; Asada, J.; Sato, K.; Hashizume, D.; Kawato, Y.; Hamashima, Y. Asymmetric Fluorolactonization with a Bifunctional Hydroxyl Carboxylate Catalyst. *J. Am. Chem. Soc.* **2015**, *137*, 10132−10135.

(12) Ota, Y.; Kawato, Y.; Egami, H.; Hamashima, Y. Enantioselective Allyl-, and Allenylboration of Aldehydes Catalyzed by Chiral Hydroxyl Carboxylic Acid. *Synlett* **2017**, *28*, 976−980.

(13) Felzmann, W.; Castagnolo, D.; Rosenbeiger, D.; Mulzer, J. Crotylation versus Propargylation: Two Routes for the Synthesis of the C13−C18 Fragment of the Antibiotic Branimycin. *J. Org. Chem.* **2007**, *72*, 2182−2186.

(14) Calder, E. D. D.; Sutherland, A. Enantioselective Synthesis of 3-Methyleneindan-1-Ols via a One-Pot Allylboration−Heck Reaction of 2-Bromobenzaldehydes. *Org. Lett.* **2015**, *17*, 2514−2517.

(15) Jain, P.; Antilla, J. C. Chiral Brønsted Acid-Catalyzed Allylboration of Aldehydes. *J. Am. Chem. Soc.* **2010**, *132*, 11884−11886.

(16) Jain, P.; Wang, H.; Houk, K. N.; Antilla, J. C. Brønsted Acid Catalyzed Asymmetric Propargylation of Aldehydes. *Angew. Chem., Int. Ed.* **2012**, *51*, 1391−1394.

(17) Grayson, M. N.; Pellegrinet, S. C.; Goodman, J. M. Mechanistic Insights into the BINOL-Derived Phosphoric Acid-Catalyzed Asymmetric Allylboration of Aldehydes. *J. Am. Chem. Soc.* **2012**, *134*, 2716−2722.

(18) Grayson, M. N.; Goodman, J. M. Understanding the Mechanism of the Asymmetric Propargylation of Aldehydes Promoted by 1,1′-Bi-2-Naphthol-Derived Catalysts. *J. Am. Chem. Soc.* **2013**, *135*, 6142−6148.

(19) Wang, H.; Jain, P.; Antilla, J. C.; Houk, K. N. Origins of Stereoselectivities in Chiral Phosphoric Acid Catalyzed Allylborations and Propargylations of Aldehydes. *J. Org. Chem.* **2013**, *78*, 1208−1215.

(20) Li, Y.; Houk, K. N. Transition Structures for the Allylboration Reactions of Formaldehyde by Allylborane and Allylboronic Acid. *J. Am. Chem. Soc.* **1989**, *111*, 1236−1240.

(21) Sakata, K.; Fujimoto, H. Quantum Chemical Study of Lewis Acid Catalyzed Allylboration of Aldehydes. *J. Am. Chem. Soc.* **2008**, *130*, 12519−12526.
(22) Grayson, M. N.; Yang, Z.; Houk, K. N. Chronology of CH···O Hydrogen Bonding from Molecular Dynamics Studies of the Phosphoric Acid-Catalyzed Allylboration of Benzaldehyde. *J. Am. Chem. Soc.* **2017**, *139*, 7717−7720.
(23) Johnston, R. C.; Cheong, P. H. Y. C-H···O Non-Classical Hydrogen Bonding in the Stereomechanics of Organic Transformations: Theory and Recognition. *Org. Biomol. Chem.* **2013**, *11*, 5057−5064.
(24) Corey, E. J.; Lee, T. W. The Formyl C−H···O Hydrogen Bond as a Critical Factor in Enantioselective Lewis-Acid Catalyzed Reactions of Aldehydes. *Chem. Commun.* **2001**, *No. 15*, 1321−1329.
(25) Terada, M.; Soga, K.; Momiyama, N. Enantioselective Activation of Aldehydes by Chiral Phosphoric Acid Catalysts in an Aza-Ene-Type Reaction between Glyoxylate and Enecarbamate. *Angew. Chem., Int. Ed.* **2008**, *47*, 4122−4125.
(26) Rodríguez, E.; Grayson, M. N.; Asensio, A.; Barrio, P.; Houk, K. N.; Fustero, S. Chiral Brønsted Acid-Catalyzed Asymmetric Allyl-(Propargyl)Boration Reaction of Ortho-Alkynyl Benzaldehydes: Synthetic Applications and Factors Governing the Enantioselectivity. *ACS Catal.* **2016**, *6*, 2506−2514.
(27) Hohenberg, P.; Kohn, W. Inhomogeneous Electron Gas. *Phys. Rev.* **1964**, *136*, B864−871.
(28) Kohn, W.; Sham, L. J. Self-Consistent Equations Including Exchange and Correlation Effects. *Phys. Rev.* **1965**, *140*, A1133−1138.
(29) Frisch, M. J.; Trucks, G. W.; Schlegel, H. B.; Scuseria, G. E.; Robb, M. A.; Cheeseman, J. R.; Scalmani, G.; Barone, V.; Mennucci, B.; Petersson, G. A.; Nakatsuji, H.; Caricato, M.; Li, X.; Hratchian, H. P.; Izmaylov, A. F.; Bloino, J.; Zheng, J.; Sonnenberg, J. L.; Hada, M.; Ehara, M.; Toyota, K.; Fukuda, R.; Hasegawa, J.; Ishida, M.; Nakajima, T.; Honda, Y.; Kitao, O.; Nakai, H.; Vreven, T.; Montgomery, J. A.; Peralta, J. E.; Ogliaro, F.; Bearpark, M.; Heyd, J. J.; Brothers, E.; Kudin, K. N.; Staroverov, V. N.; Kobayashi, R.; Normand, J.; Raghavachari, K.; A. Rendell, J. C.; Burant, S.; Iyengar, S.; Tomasi, J.; Cossi, M.; Rega, N.; Millam, J. M.; Klene, M.; Knox, J. E.; Cross, J. B.; Bakken, V.; Adamo, C.; Jaramillo, J.; Gomperts, R.; Stratmann, R. E.; Yazyev, O.; Austin, A. J.; Cammi, R.; Pomelli, C.; Ochterski, J. W.; Martin, R. L.; Morokuma, K.; Zakrzewski, V. G.; Voth, G. A.; Salvador, P.; Dannenberg, J. J.; Dapprich, S.; Daniels, A. D.; Farkas, O.; Foresman, J. B.; Ortiz, J. V.; Cioslowski, J.; Fox, D. J. *Gaussian 9*, Revision D.01; Gaussian, Inc.: Wallingford CT, 2009.
(30) Frisch, M. J.; Trucks, G. W.; Schlegel, H. B.; Scuseria, G. E.; Robb, M. A.; Cheeseman, J. R.; Scalmani, G.; Barone, V.; Mennucci, B.; Petersson, G. A.; Nakatsuji, H.; Caricato, M.; Li, X.; Hratchian, H. P.; Izmaylov, A. F.; Bloino, J.; Zheng, J.; Sonnenberg, J. L.; Hada, M.; Ehara, M.; Toyota, K.; Fukuda, R.; Hasegawa, J.; Ishida, M.; Nakajima, T.; Honda, Y.; Kitao, O.; Nakai, H.; Vreven, T.; Montgomery, J. A.; Peralta, J. E.; Ogliaro, F.; Bearpark, M.; Heyd, J. J.; Brothers, E.; Kudin, K. N.; Staroverov, V. N.; Kobayashi, R.; Normand, J.; Raghavachari, K.; A. Rendell, J. C.; Burant, S.; Iyengar, S.; Tomasi, J.; Cossi, M.; Rega, N.; Millam, J. M.; Klene, M.; Knox, J. E.; Cross, J. B.; Bakken, V.; Adamo, C.; Jaramillo, J.; Gomperts, R.; Stratmann, R. E.; Yazyev, O.; Austin, A. J.; Cammi, R.; Pomelli, C.; Ochterski, J. W.; Martin, R. L.; Morokuma, K.; Zakrzewski, V. G.; Voth, G. A.; Salvador, P.; Dannenberg, J. J.; Dapprich, S.; Daniels, A. D.; Farkas, O.; Foresman, J. B.; Ortiz, J. V.; Cioslowski, J.; Fox, D. J.. *Gaussian 16*, Revision A.03; Gaussian, Inc.: Wallingford CT, 2016.
(31) McCoy, L. L.; Mal, D. Intramolecular Hydrogen Bonding and Acidity of Some γ-Hydroxy- and γ-Methoxy-α,β-Unsaturated Carboxylic Acids. *J. Org. Chem.* **1984**, *49*, 939−942.
(32) Pedregal, J. R.-G.; Gómez-Orellana, P.; Maréchal, J.-D. ESIgen: Electronic Supporting Information Generator for Computational Chemistry Publications. *J. Chem. Inf. Model.* **2018**, *58*, 561−564.

https://dx.doi.org/10.1021/acs.joc.0c02226
J. Org. Chem. 2020, 85, 15449−15456